



ELSEVIER

Tectonophysics 354 (2002) 101–119

TECTONOPHYSICS

www.elsevier.com/locate/tecto

# Pull-apart formation and strike-slip partitioning in an obliquely divergent setting, Leka Ophiolite, Norway

S.J. Titus<sup>a,\*</sup>, H. Fossen<sup>b</sup>, R.B. Pedersen<sup>b</sup>, J.L. Vigneresse<sup>c</sup>, B. Tikoff<sup>a</sup>

<sup>a</sup>Department of Geology and Geophysics, University of Wisconsin, 1215 West Dayton Street, Madison, WI 53706, USA

<sup>b</sup>Department of Geology, University of Bergen, Allégaten 41, N-5007 Bergen, Norway

<sup>c</sup>CREGU, UMR CNRS 7566 G2R, BP 23, F-54501 Vandoeuvre-Nancy, France

Received 12 October 2001; accepted 29 May 2002

## Abstract

The Leka Ophiolite Complex (LOC) is located on the island of Leka, Norway, and belongs to the Uppermost Allochthon of the Scandinavian Caledonides. The rocks of the adjacent mainland and most of the surrounding islands are basement gneisses and supracrustal rocks not related to the ophiolite complex. Paleostress analysis, gravity inversion, and regional geology support a fault-bounded rhombochasm geometry for the LOC. The paleostress inversions revealed two types of tensors, interpreted as small strains: (1) horizontal extension, generally E–W to NE–SW, and (2) horizontal extension in the same direction with an added component of perpendicular horizontal contraction. A strong positive gravity anomaly (25 mGal) is centered on Leka, and gravity inversion indicates that the LOC lies directly below its surface exposures with steep-sided walls and a flat bottom located at  $\sim 7$  km depth. The faults bounding the LOC probably initiated during postorogenic extension in the Scandinavian Caledonides. The faults are regional in scale and are parallel to other NE–SW trending en echelon faults along the Norwegian coastline and on the adjacent mainland.

A pull-apart structure explains the down-dropping and subsequent preservation of the LOC, as it is surrounded by rocks from lower structural positions within the nappe stack. The paleostress directions from Leka support a sinistral component of shear along these faults. The gravity inversion is consistent with a fault-bounded geometry. This pull-apart structure, as uniquely recorded by the dense ophiolitic rocks, suggests that strike-slip partitioning was active in an obliquely divergent setting.

© 2002 Elsevier Science B.V. All rights reserved.

*Keywords:* Extension tectonics; Pull-apart structures; Ophiolite; Leka Island, Nord-Trøndelag, Norway; Caledonides

## 1. Introduction

Pull-apart geometries are well cited in the geological literature, resulting from either a discrete break (dilation jog) or bend (releasing bend) in a strike-slip fault system. Pull-apart geometries may be segmented,

such as the case for a strike-slip duplex, or exist as a single cavity. Pull-apart structures are generally inferred to occur as basins (Sylvester, 1988), although centimeter-scale veins (e.g., Peacock and Sanderson, 1995), region-scale plutons (e.g., Tikoff and Teysier, 1992), and regional-scale blueschist massifs (e.g., Mann and Gordon, 1996) are also inferred to fill these structural “holes” (Aydin and Nur, 1982).

The map-view expression of these structures is well known, such as the typical aspect 3:1 (length/

\* Corresponding author. Fax: +1-608-262-0693.

E-mail address: stitus@geology.wisc.edu (S.J. Titus).

width) ratio in plan view (Aydin and Nur, 1982). However, much less is known about the three-dimensional geometries of pull-aparts. The difficulty is that it is rarely possible to observe an entire pull-apart structure, and certainly not one on a crustal scale. Moreover, it is often difficult to know the kinematics or dynamics *within* the pull-apart structure, as it is often filled by unconsolidated sediments, crystallizing materials (veins/plutons), or highly structurally disrupted material (blueschists).

We present the results of our study of the Leka Ophiolite Complex (LOC), western Norway. We infer, on the basis of regional geology, that the LOC is a down-faulted block in a pull-apart strike-slip setting. Paleostress analyses of striated fault surfaces are used to evaluate the orientation of stresses within this pull-apart setting and are consistent with sinistral bounding faults. The densities of the mafic and ultramafic rocks, relative to the surrounding gneisses, allow us to evaluate the depth and shape of the pull-apart geometry. The LOC is bounded by steep walls and has a relatively flat bottom at  $\sim 7$  km depth, consistent with a pull-apart setting.

In addition to information about pull-apart geometries, we use this structure to evaluate the nature of orogenic collapse in the Scandinavian Caledonides. The pull-apart geometry is a clear indication of orogen-parallel, strike-slip motion, which presumably occurred during late-stage extension. The existence of the LOC, which is uniquely tied to the highest known level of thrust sheets in the Scandinavian Caledonides, indicates a transcurrent component of deformation during postorogenic extension. Consequently, we first briefly summarize the regional geology. We then review the paleostress analysis and three-dimensional gravity inversion before discussing the implications of our study.

## 2. General setting of Leka Ophiolite Complex

### 2.1. *Obduction and postorogenic extension*

The Scandinavian Caledonides are composed of a series of thrust sheets emplaced onto the autochthonous crystalline basement of the Baltic shield. The thrust sheets are named for their relative position in the nappe stack as the Parautochthon, Lower, Mid-

dle, Upper, and Uppermost Allochthons. A critical aspect of the structurally high thrust sheets (Upper and Uppermost Allochthons) is the occurrence of many ophiolites and island-arc complexes (e.g., Hossack and Cooper, 1986; Milnes et al., 1997). The contractional deformation in western Norway occurred in island-arc settings during the Ordovician to Early Silurian closing of the proto-Atlantic Iapetus ocean and continued during the Late Silurian to Early Devonian continent–continent collision (e.g., Roberts and Gee, 1985). Mild post-Caledonian contraction (transpression) of possible Late Devonian Period are found in restricted areas (e.g., Braathen, 1999; Krabbendam and Dewey, 1998). Most of the translation of the allochthonous thrust sheets occurred during the Scandinavian orogeny with a minimum of 400 km of shortening (Hossack and Cooper, 1986).

Postorogenic extension began immediately following collision during the Early Devonian Period (Fossen, 1992, 2000; Andersen, 1998; Terry et al., 2000). Movement occurred both as backsliding along preexisting thrust sheets, Mode I extension, and as higher-angle, listric normal faults, Mode II extension (Fossen, 1992; Milnes et al., 1997). The formation of Devonian basins, such as the Hornelen basin, is associated with the normal faults (Steel et al., 1985; Osmundsen et al., 1998; Osmundsen and Andersen, 2001). Mesozoic opening of the North Atlantic also produced extensional structures, which are well-studied offshore Norway (e.g., Gabrielsen et al., 1984).

Large strike-slip zones became active locally in the coastal areas of Norway during extension. A well-studied example is the Møre–Trøndelag fault zone (Fig. 1), which forms the northern margin of the Western Gneiss Region (Grønlie and Roberts, 1989; Séranne, 1992; Krabbendam and Dewey, 1998). This strike-slip zone had left-lateral movement during the Devonian Period (e.g., Séranne, 1992) but has a long deformation history (e.g., Grønlie et al., 1994). This feature followed a preexisting Caledonian structure, presumably related to the original margin of Baltica. The Møre–Trøndelag fault zone served as a transfer zone in the Devonian Period between extensional detachments presently offshore and low-angle detachments of the onshore Devonian basins (Séranne, 1992; Gabrielsen et al., 1999).

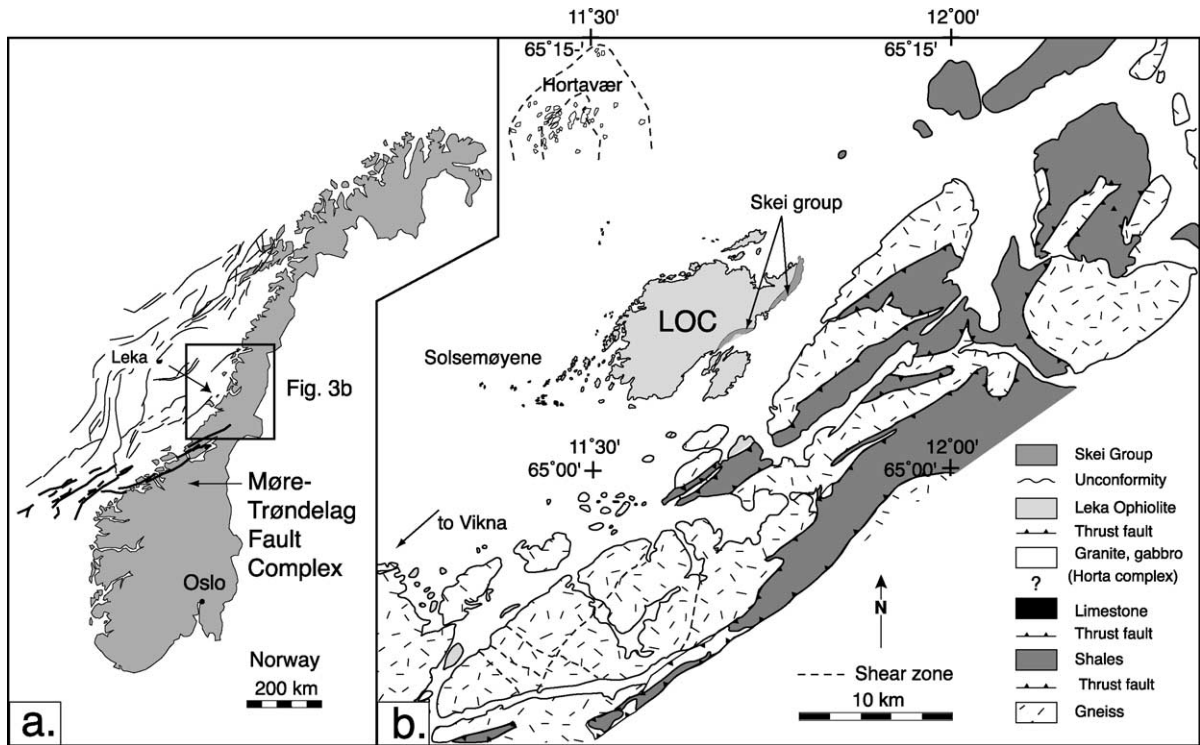


Fig. 1. (a) Map of Norway, showing the location of Leka and major offshore and onshore faults. (b) Regional geology of Nord-Trøndelag. The rocks of the adjacent mainland, and Vikna area, are gneisses from structurally lower positions within the Caledonian nappe stack. The rocks to the NNW of Leka are granites and gabbros of the Horta complex, which are from the Middle Allochthon. Limestones and sandstones make up the Solsemøyene group, also not related to the LOC though its exact stratigraphic position is unknown.

## 2.2. Regional setting of the Leka Ophiolite Complex

The LOC is located at  $\sim 65^\circ\text{N}$  on the western edge of the Trøndelag platform. It is believed that many of the Scandinavian ophiolites, including the LOC, were accreted onto the Laurentian margin during the Taconic orogeny and subsequently transferred to Baltica during the continent–continent collision (Pedersen et al., 1988).

In this region, ophiolite complexes are present in the Upper and Uppermost Allochthons, which is also the probable tectonostratigraphic position of the LOC. Basement gneisses of the northern Vestranden region (Folda–Vikna area), which are metamorphosed to amphibolite grade, outcrop south and west of Leka. These gneisses also form the dominant rock type on the adjacent mainland. Cambro-Silurian metasediments, interpreted as belonging to the Middle Allochthon, outcrop to the west and north of Leka. There are no

exposed contacts between the LOC and these surrounding rocks (Furnes et al., 1988), which are both structurally and stratigraphically unrelated to the LOC (Fig. 1).

The lack of continuity between Leka and surrounding rocks suggests all contacts are tectonic. Furnes et al. (1988) inferred a set of shear zones or faults closely bounding the island to the south and west, because the meta-limestones and sandstones of the Solsemøyene Group on nearby islets are not associated with the ophiolite complex. A tectonic contact is also inferred between the LOC and the gneisses to the east and south. Since rocks belonging to the Middle Allochthon, Lower Allochthon, and Parautochthon surround the LOC, it is presently in an unusually low structural position.

## 2.3. Leka Ophiolite Complex

The LOC is found only on Leka, a 90-km<sup>2</sup> island, and immediately surrounding islands (Fig. 2). The

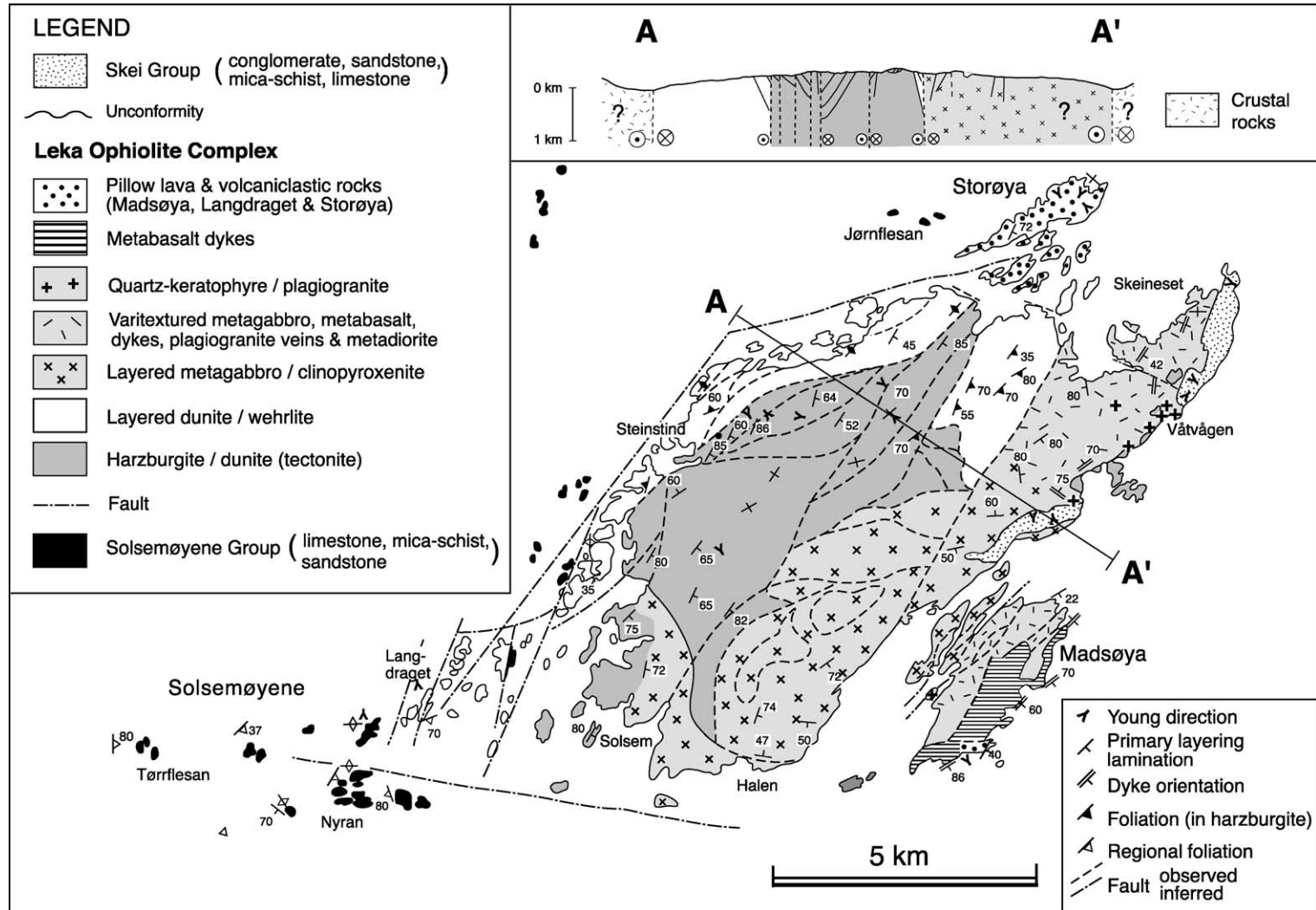


Fig. 2. Geological map and cross-section of Leka. The Leka Ophiolite Complex consists of a nearly complete ophiolite section, including pillow basalt and sediments (northeast side of island), sheeted dikes (Madsøya), gabbros (east side of Leka), and ultramafic rocks (west side of Leka). The cross-section shows the steeply dipping foliation of the mafic and ultramafic sections, cut by subvertical faults. Modified from Furnes et al. (1988).

ophiolite has one of the largest ultramafic sections in Scandinavia (Prestvik, 1972; Pedersen, 1986; Furnes et al., 1988) with an age of  $497 \pm 2$  Ma based on U/Pb on zircons from plagiogranites (Dunning and Pedersen, 1988). Ordovician metasedimentary rocks (Skei Group) were deposited nonconformably on the ophiolite and metamorphosed in a tight syncline in the NE portion of the island (Sturt et al., 1985).

The LOC has undergone regional metamorphism as well as multiple deformation events. Metamorphic grade reaches at least greenschist facies with some evidence of relict amphibolite facies in the gabbroic rocks (Prestvik, 1972). On a large scale, the ultramafic and mafic units are folded into two open synclines separated by a later-stage fault (see cross-section in Fig. 3). Foliation measurements across the large syncline indicate that the fold hinge plunges moderately to the NE. Several tight folds within the ultramafic unit define moderate-scale ductile deformation, observable in both aerial photos and in the field. The hinge lines of these folds plunge steeply to the NE.

A later stage (or stages?) of brittle deformation affected the LOC, as evidenced by numerous faults

that crisscross the island on varying scales. Several large-scale faults, trending NE–SW, split the LOC into discrete blocks. In addition to the large faults, many moderate size faults are visible on air photos as linear features unaffected by topography, indicating that they are subvertical.

### 3. Paleostress analysis

#### 3.1. Fault populations

Aerial photographs reveal two distinct fault sets on Leka, a NE–SW orientation for the larger/longer faults and a NW–SE orientation for smaller/shorter faults (Fig. 3). Both sets of fault orientations are also observed in the field. The large NE–SW-oriented faults do not offset or distort the stratigraphy in any predictable way, making it difficult to determine the extent of the strike-slip or dip-slip components. No offset markers were observed on the large NE–SW faults, whereas the smaller faults exhibit minor shear displacements.

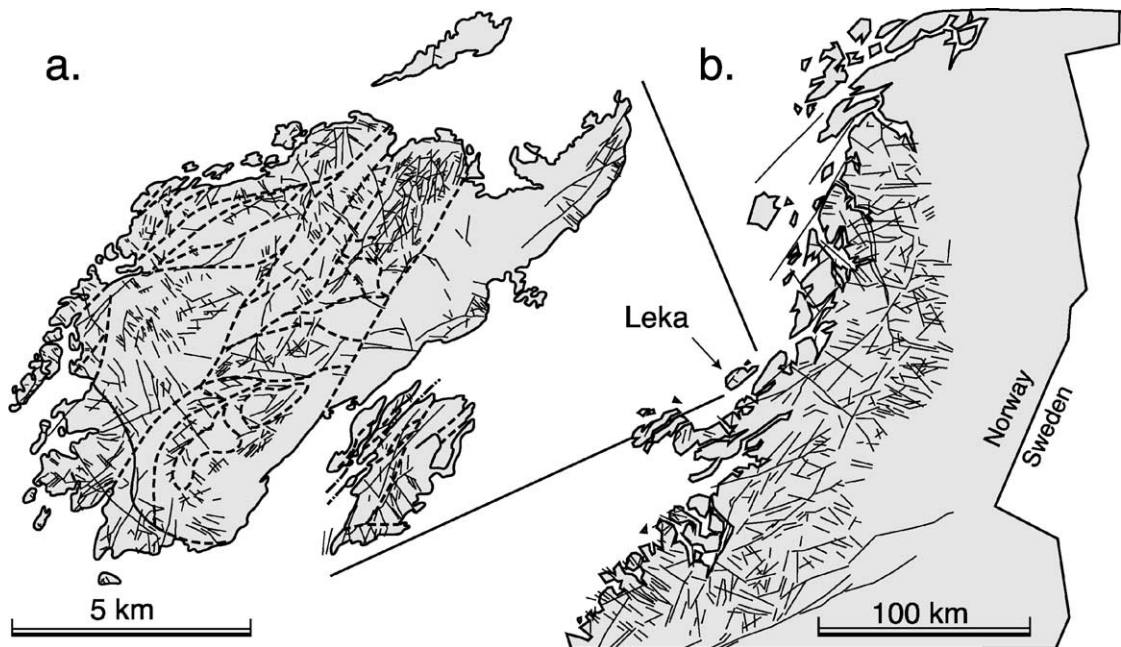


Fig. 3. (a) Lineament map of Leka. There is a predominance of NE–SW-oriented lineaments, which are identified as faults in the field, and often offset on different structural domains. Shorter faults trend NW–SE and many show sinistral offset. (b) Regional map shows the predominance of long coast-parallel, NE-oriented lineaments, and shorter NW–SE-oriented lineaments.

In outcrop, the fault surfaces have coatings of serpentine mineral that were polished and striated during slippage. Calcite is locally precipitated on the slip surfaces and generally Riedel-type fracture development (Hancock, 1985; Petit, 1987) created steps with growth of fibrous serpentine or precipitation of calcite, clearly indicating the local sense of slip. Some fault planes showed multiple phases of mineral growth, suggesting that these faults were reactivated. However, there were no consistent crosscutting relationships on the fault surfaces or between faults at a particular site, and, therefore, no constraints exist on the relative timing of the movements.

Our data set consists of 670 fault and striae orientations, with the sense of motion, from mesoscopic faults at 25 locations across both Leka and the neighboring Madsøya. The study sites are from the mafic and ultramafic sections of the ophiolite complex. In general, ultramafic rocks are very good recorders of fault slip, because the fault planes commonly contain slickensides (e.g., Wojtal, 2001). However, ultramafic rocks deform in a brittle manner to relatively large crustal depths and high temperatures relative to granitic or sedimentary rocks. They also act as competent units and therefore concentrate stress (e.g., Hibbard, 1983). Consequently, the studied ultramafic rocks are particularly susceptible to fault movement and probably record most regional deformational events.

### 3.2. Methodology

Paleostress inversion techniques have been used by various workers for more than 20 years. They are based upon the work of Wallace (1951) and Bott (1959), who suggested that slip on faults is parallel to the maximum resolved shear stress. We will only briefly discuss the underlying assumptions and method of paleostress inversions, as this is discussed in detail elsewhere (e.g., Etchecopar et al., 1981; Angelier et al., 1982; Michael, 1984; Angelier, 1994). The purpose of the paleostress inversion is to determine a stress tensor for a given set of fault and striae orientations. Usually, this data is the reduced stress tensor, which is defined by four unknowns: the orientations of the three principal stress axes  $\sigma_1$ ,  $\sigma_2$ , and  $\sigma_3$  (where  $\sigma_1 \geq \sigma_2 \geq \sigma_3$ ) and the tensor aspect ratio  $R$ , where  $R = (\sigma_1 - \sigma_2) / (\sigma_1 - \sigma_3)$  (Célérier, 1988). Note that the ratio  $R$  is slightly different than the parameter  $\phi$  defined by Angelier (1975, 1989). The

analysis is valid when the following assumptions are met: (1) the faults are in an isotropic medium; (2) the stress tensor is symmetric and the stress state is homogeneous for the area; and (3) the shear force applied on a fault plane is parallel to the movement along that plane (Etchecopar et al., 1981). In addition, it is important that the measured faults have a variety of orientations so the stress tensor is better constrained.

There are some questions, pointed out by various workers, about the validity and applicability of paleostress analysis. First, brittle deformation can result in complicated and linked systems of faults that interact and cause local perturbations in the stress field. Second, slip along a fault surface may not be parallel to the shear stress. These two concerns were addressed by Angelier (1994). Numerical modeling indicates that changes in the stress field, resulting from the above conditions, are less than uncertainties in the data collection itself. A third concern is the degree to which one must adhere to the basic assumptions of paleostress analysis (isotropic material and homogeneous stress conditions). Wojtal and Pershing (1991) demonstrated that some conditions may be violated and robust reduced stress tensors are still produced. Finally, there is discussion whether the paleostress principal directions model stress or incremental strain rates (Wojtal and Pershing, 1991; Twiss and Unruh, 1998). We acknowledge that fault arrays fundamentally record incremental strain, although this data can be interpreted as paleostress if the conditions outlined by Etchecopar et al. (1981) are met.

The majority of the data were analyzed using Célérier's (1999) computer program FSA (version 18), one of many programs available that solve the inverse problem through various statistical approaches (e.g., Etchecopar et al., 1981; Angelier, 1984; Michael, 1984; Reches, 1987; Will and Powell, 1991; Nemcock and Lisle, 1995). FSA generates a large number of reduced stress tensors by a random grid search. The reduced stress tensor is used to calculate the predicted slip for each fault, which is then compared to the actual slip on each fault plane. The angular difference between these two values, called the misfit angle, is used as a measure of how well the tensor solution fits the actual data.

Our procedure was to invert a population of faults from a single site. Those faults with large misfit angles, greater than  $45^\circ$ , were rejected, and the inversion pro-

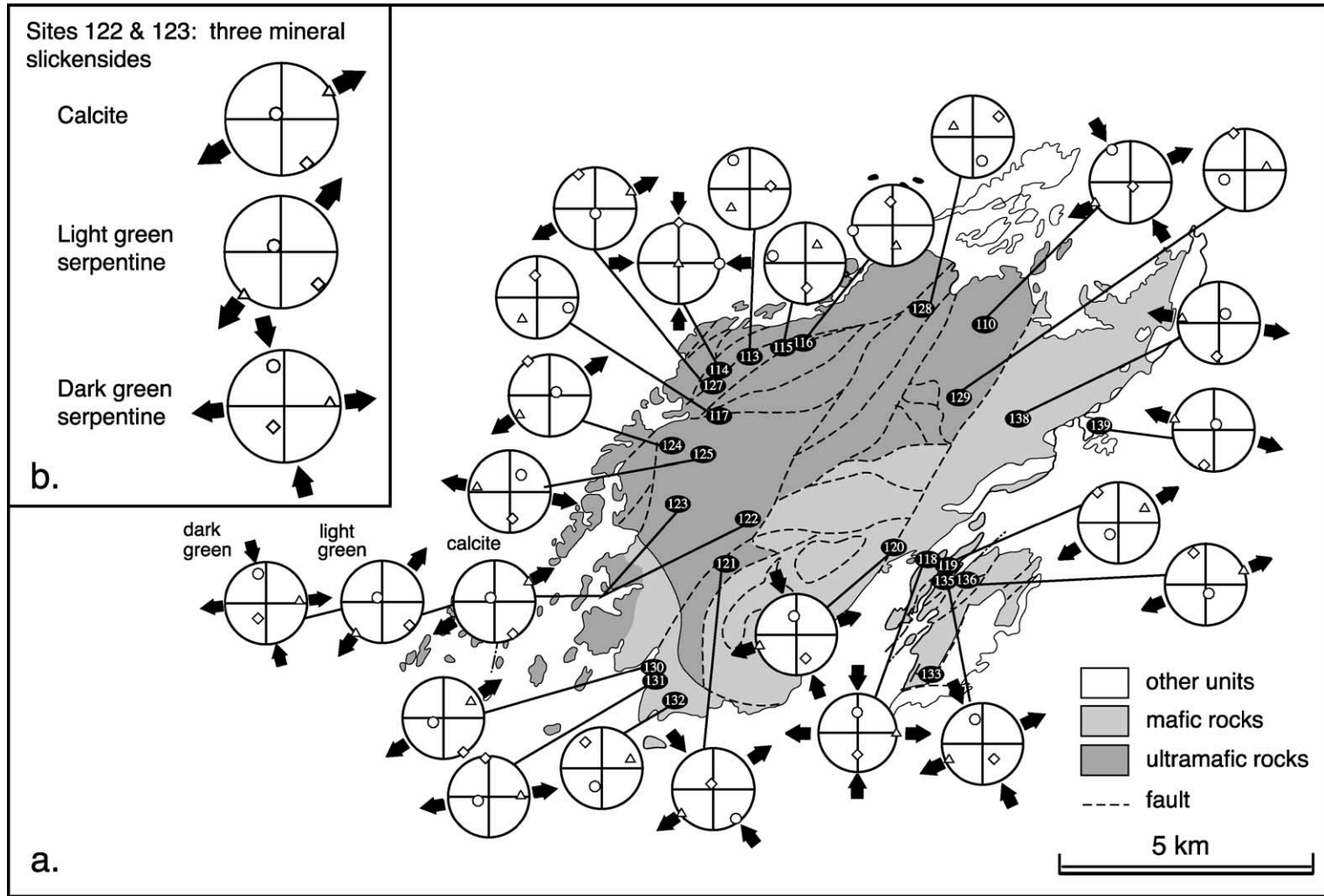


Fig. 4. (a) Map of Leka with superimposed stress tensors. The stress tensors are denoted by the lower hemisphere, stereonet projections where circle =  $\sigma_1$ , diamond =  $\sigma_2$ , triangle =  $\sigma_3$ . The three types correspond to: (1) horizontal tension (outward arrows only); (2) horizontal compression and tension (outward and inward arrows); and (3) obliquely oriented stress axes (no arrows). For the former two types, tension is generally oriented EW to NE and compression is oriented NS to NNW. (b) Inset shows the inversions for the three discrete populations of slickenside fibers at Sites 122 and 123. See text for details.

gram was rerun. This process was repeated until we obtained a group of faults with one homogeneous solution. In all cases, there were at least nine faults remaining per site (five is considered the minimum number), and in most cases, the stress tensor was based on at least 60% of the original fault data (see Appendix A for details). The discarded data from each site were rerun through the inversion process in an attempt to separate multiple deformation events. However, this resulted in: (1) too few faults ( $n < 5$ ) remaining after one iteration; (2) tensors with oblique slip axes; or (3) in two cases, meaningful stress tensors were resolvable, but these simply recorded the “other” stress tensor type of the two types that were distinguished (see Section 3.3).

### 3.3. Results

We found considerable variation in stress tensors from Leka (Fig. 4). However, visual sorting of the inversion results revealed two main types of stress tensors. One set, with 11 locations distributed throughout the island, shows pure tension that varies from E–W to NE–SW. A second group of data, located at six sites predominately on the SE side of the island, exhibited the same tension direction with an added component of perpendicular, horizontal compression. Some localities show both types of tensors. Overall, the tension direction is predominately ENE–WSW. Three sites do not correspond to this trend and indicate ESE–WNW tension. Two of these sites are adjacent to one another and are located in the NE part of the island, while the third site has less well-defined stress directions (Station 125). In all cases, contraction is dominantly NNW–SSE.

Relative dating of the two sets of stress tensors was not possible. However, we have limited evidence confirming that there were at least two episodes of deformation. This is based on data from two sites close to one another (122 and 123) that had lineations composed of three different minerals: calcite, light green serpentine, and dark green serpentine. This mineralogical information was used to combine the data from both sites and to analyze each mineral population separately (see Fig. 4b). Paleostress tensors from both the calcite and the light green serpentine slickensides are solely tensional, with NE–SW-directed tension. The paleostress tensor for the dark green serpentine has a rotated tension direction to E–W with an added component of N–S compression.

These two different tensors are consistent with our overall results for the rest of the island and indicate that there were at least two phases of deformation. We did not observe consistent overprinting relationships between these different minerals in the field. Therefore, it is not possible to infer relative timing from the tensor variations that relate to a particular type of slickenside.

There are seven sites that show oblique stress axes. Many of these are in the NW part of the island. At this locality, the sites are adjacent to a major fault. Possible reasons for this pattern include the reactivation of the major fault during multiple events, or local adjustments and deviations in a paleostress field.

## 4. Gravity survey and interpretation

### 4.1. Gravity measurements

Sindre and Pedersen (1990) conducted a gravity survey of the LOC with 130 measurements on Leka and 374 measurements on the surrounding islands and mainland. The gravity data were corrected for elevation, latitude, and terrain with an overall elevation precision on the order of  $\sim 1$ – $3$  m, corresponding to  $0.3$ – $1$  mGal. The estimated errors on the Bouguer anomaly values are  $< 1$  mGal. The corresponding Bouguer anomaly map (Fig. 5a) indicates a 25-mGal positive anomaly associated with the island of Leka. These very large positive values reflect the density of ultramafic rocks in contrast to the surrounding gneisses and sediments.

### 4.2. 3D Inversion methodology

In order to compute the three-dimensional gravity inversion, we used an iterative inversion technique modified from the original Cordell and Henderson (1968) method. This method uses the Bouguer anomaly as the basis for the inversion and is described in detail by Vigneresse (1990). The regional field gradient, caused by the transition from continental to oceanic crust along the coastline, is removed from the Bouguer anomaly, and the data are then inverted.

The inversion process relies on the density contrast between the LOC and the surrounding rocks. In this case, we employed a density of  $3.1$  g/cm<sup>3</sup> for the ultramafic rocks and  $2.7$  g/cm<sup>3</sup> for the surrounding gneisses for the inversion. These average values are in



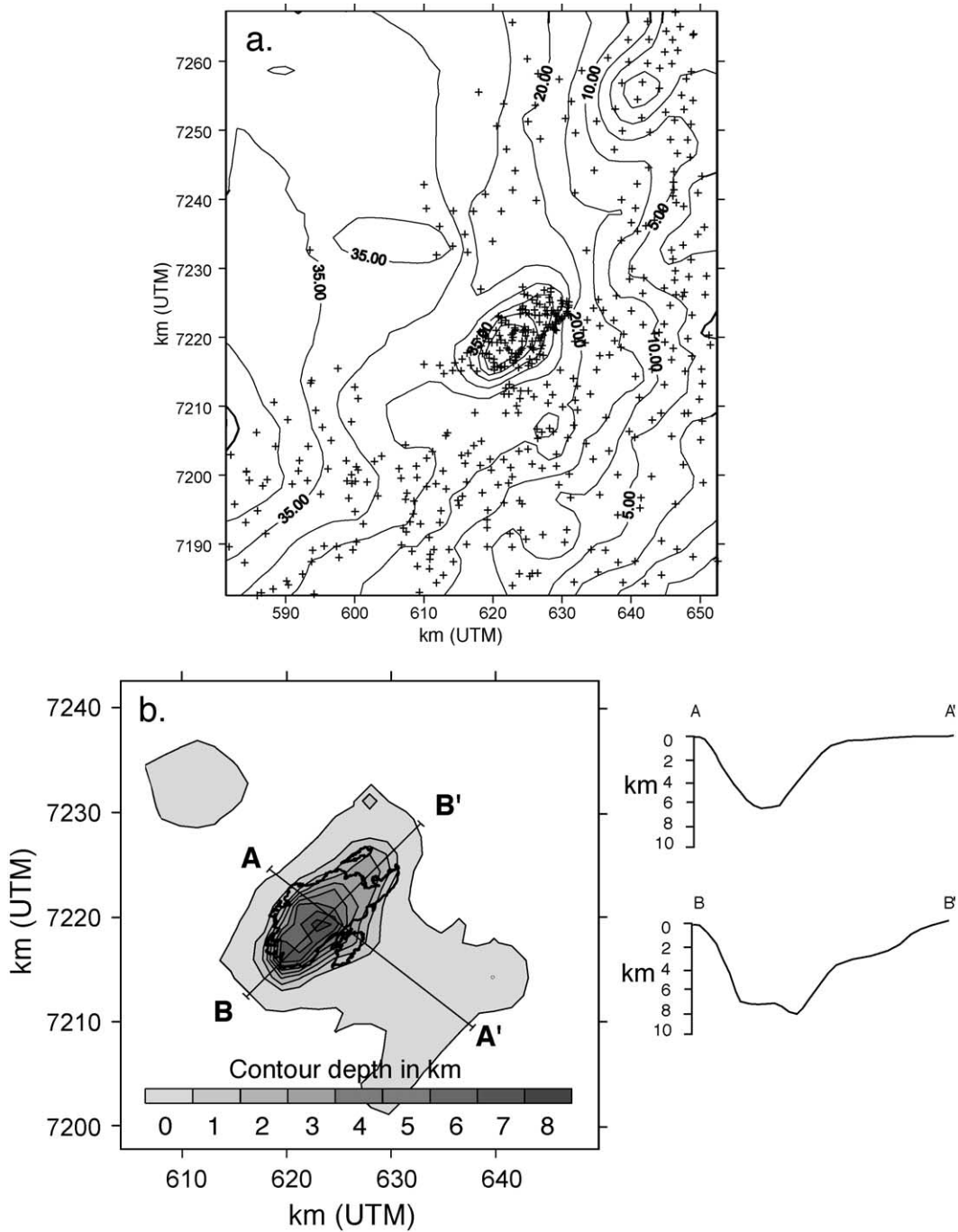


Fig. 5. (a) Bouguer anomaly map of Leka from the data of *Sindre and Pedersen (1990)*. The contour interval is 5 mGal, and the axes are in UTM (Universal Transverse Mercator) coordinates. The LOC is demarcated by a closed-contour, positive 25-mGal anomaly. (b) Results of the gravity inversion with the outline of the LOC superimposed. The inversion and two cross-sections show a steep-walled body with a flat bottom at  $\sim 7$  km depth.

accord with the 22 samples from Leka measured by [Sindre and Pedersen \(1990\)](#). Thus, the inferred density contrast is  $0.4 \text{ g/cm}^3$  and is assumed as being constant throughout the field area. The variation of the rock density with depth is assumed to be similar in both the ultramafic rocks and in the surrounding gneisses and is therefore a second-order effect that may be ignored (e.g., [Améglio et al., 1996](#)). Additionally, a series of tests using variable density contrasts is performed in order to infer the error on the depth.

#### 4.3. Results

A simple first-order picture of the LOC results from the inversion ([Fig. 5b](#)) where the ophiolite has a rhombochasm geometry with steep walls and a flat bottom. The body's greatest thickness is approximately  $\sim 6\text{--}8$  km, similar to the results of the previous two-dimensional model ([Sindre and Pedersen, 1990](#)). The maximum thickness corresponds to the area from the center of Leka towards the SW part of the island. The precision of the thickness was tested by varying the density contrast by  $\pm 0.05 \text{ g/cm}^3$ . We consider that the total uncertainty of the calculated depth, due to both measurement errors and the inversion process, does not exceed  $\pm 16\%$ .

The walls are steepest on the NW and SW sides of the body. The walls are relatively steep on the SE side of the LOC, but slightly less so than the SW and NW side. Gabbroic rocks, rather than ultramafic rocks, are found predominantly on the E side of the island. The occurrence of gabbros at the surface in the east would tend to lower the gradient and decrease the steepness for the eastern walls. The walls have the shallowest dip on the NE side of Leka. This result corresponds well to the regional geology, as the structurally higher level units of the ophiolites (pillow lavas and overlying sedimentary rocks) are found on small islands offshore to the NE. These rocks have very similar densities to the surrounding gneisses. Consequently, the walls may be equally steep on all sides of the LOC but are best displayed on the NW and SW parts of the island where the ultramafic rocks are juxtaposed against the surrounding gneisses.

## 5. Discussion

Today, the LOC has a puzzling position with respect to its surrounding rocks, which are from stratigraphi-

cally and tectonically lower positions in the nappe stack of the Scandinavian Caledonides. To understand the enigmatic position of the LOC, we combined evidence from gravity data, regional lineaments, field mapping, and paleostress analysis. We propose that the LOC lies within a dilation jog, or pull-apart, in a sinistral strike-slip fault system. This fault system parallels the Norwegian coastline and is related to the postorogenic extension in the Scandinavian Caledonides.

#### 5.1. Three-dimensional shape of the LOC

The three-dimensional shape of the LOC, determined by gravity inversion, supports the preservation of the ophiolite in a pull-apart setting. The 25-mGal positive gravity anomaly requires that the LOC extends to depth. This observation, along with the vertical orientation of primary layering in the ophiolite, suggests that the LOC is not a thin horizontal body but was tectonically modified by postemplacement deformation. The gravity inversion supports this interpretation as it confirms the vertical extent of the complex ( $\sim 7$  km). Furthermore, the steep walls and flat bottom of the body demonstrate not only a rhombochasm geometry but also the existence of faults bounding the LOC close to its surface exposures.

#### 5.2. Sinistral NE–SW bounding faults

There are four possible fault geometries that are consistent with the rhombochasm shape of the LOC ([Fig. 6a and b](#)). Major faults could run either E–W or NE–SW, and the pull-apart could result from either dextral or sinistral movement on these faults, depending on the arrangement of the overlapping sections. We have no direct evidence for which of these possible orientations of bounding faults resulted in the pull-apart geometry. However, combining the regional fracture patterns with the paleostress analysis from Leka suggests that the bounding faults are NE–SW trending with sinistral movement.

Several lines of evidence suggest that the island is bounded by NE–SW-oriented faults. First, the regional pattern of lineaments is similar to that observed on Leka ([Fig. 3b](#)). These are based on a digital elevation model and are inferred to represent the presence of fracture zones. In this case, the fracture zones that trend NE–SW are continuous and regional, whereas fracture zones

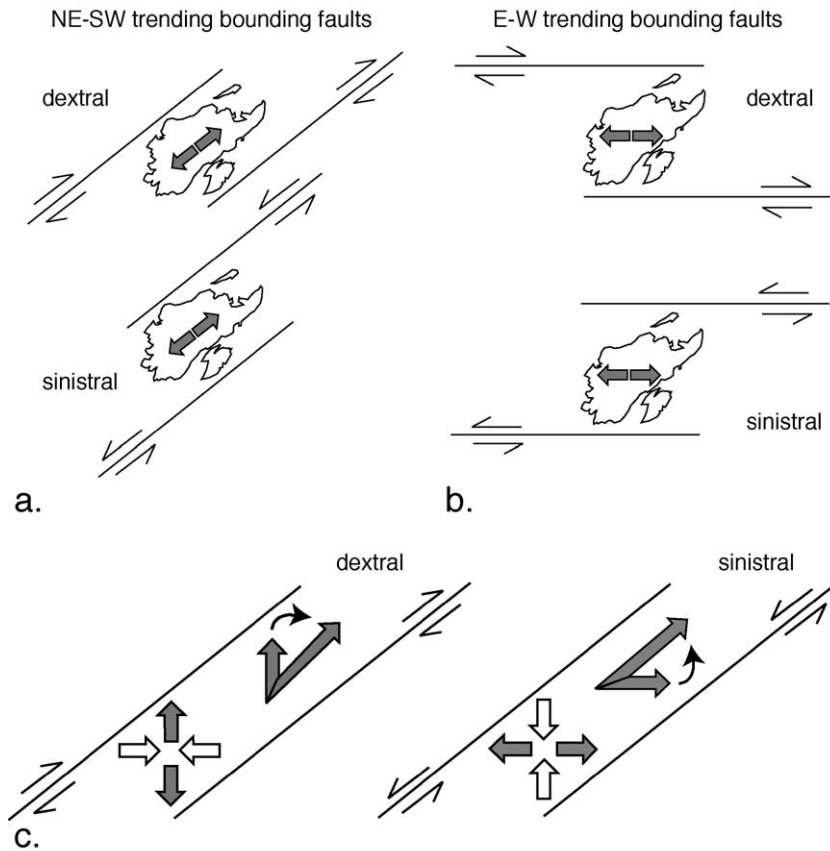


Fig. 6. The four possible pull-apart geometries to explain the rhombochasm geometry of the LOC. (a) Bounding faults oriented NE–SW. (b) Bounding faults oriented E–W. Either geometry can exist with sinistral or dextral bounding faults. (c) Sinistral and dextral wrench zones oriented NE–SW. The paleostress data supports sinistral motion along the bounding faults.

that trend NW–SE are discontinuous and shorter. Second, the coastal morphology allows for the existence of long NE–SW trending faults parallel to the long axis of the island, located in the NE–SW trending fjords of this region, whereas there is no evidence for E or SE trending faults. Third, there is a set of en echelon faults trending NE–SW along the coast from the Møre–Trøndelag fault complex and northward to the Vikna area, just south of Leka (Sollie et al., 1997). Finally, the island is longer, and the major faults on the island are oriented in the NE–SW direction.

If the major faults are trending NE–SW, the movement along the bounding faults is either dextral or sinistral (Fig. 6a). The small faults, on which offset can be documented, generally show sinistral movement. If these faults are interpreted as synthetic to

movement along the larger faults, the bounding faults are also sinistral. Alternatively, we can use paleostress analysis, done on small faults from between the large faults, to resolve this question. To do so, we will make the assumption that the infinitesimal extension direction correlates with the paleostress tension direction and the infinitesimal contraction direction correlates with the paleostress compression direction. This is the preferred method to interpret fault array data for many authors (e.g., Twiss and Unruh, 1998). In this context, the pull-apart geometry is viewed as part of a wrench zone. In a dextral system with NE–SW-oriented faults, the infinitesimal extension (tension) direction is N–S oriented (Fig. 6c). With progressive deformation, the extension direction rotates into a NE–SW orientation. In contrast, a similarly oriented sinistral system starts

with an infinitesimal extension direction oriented E–W. With progressive deformation, the finite extension is also oriented NE–SW. Our paleostress inversion is consistent with the sinistral setting for two reasons. First, the infinitesimal extension direction varies from E–W to NE–SW. Second, the infinitesimal contraction (compression) direction is dominantly oriented N–S to NNW–SSE.

### 5.3. Interpretation of faulting on Leka

We cannot constrain the age of faulting within the LOC, although it is probably related to the latest stage of orogenic extension for several reasons. First, the faults clearly postdate the folding of the ophiolite layering.

Second, the slip surfaces measured are all purely brittle structures with no signs of ductile reactivation as might be observed in the main phase of the Caledonian orogeny. Third, the extension direction on Leka is parallel to the extension direction observed regionally (Braathen et al., 2000). Fourth, orogenic extension represents the last major tectonic episode on the mainland in western Norway. Fifth, although Mesozoic extension occurred in western Norway, it recorded different kinematics than Late Paleozoic extension. Séranne (1992) speculates on the occurrence of large (> 50 km) sinistral movements along the Møre–Trøndelag fault zone during the Late Devonian Period. Sinistral, margin-parallel motion has been documented by other workers as well (e.g. Buckovics et al., 1984;

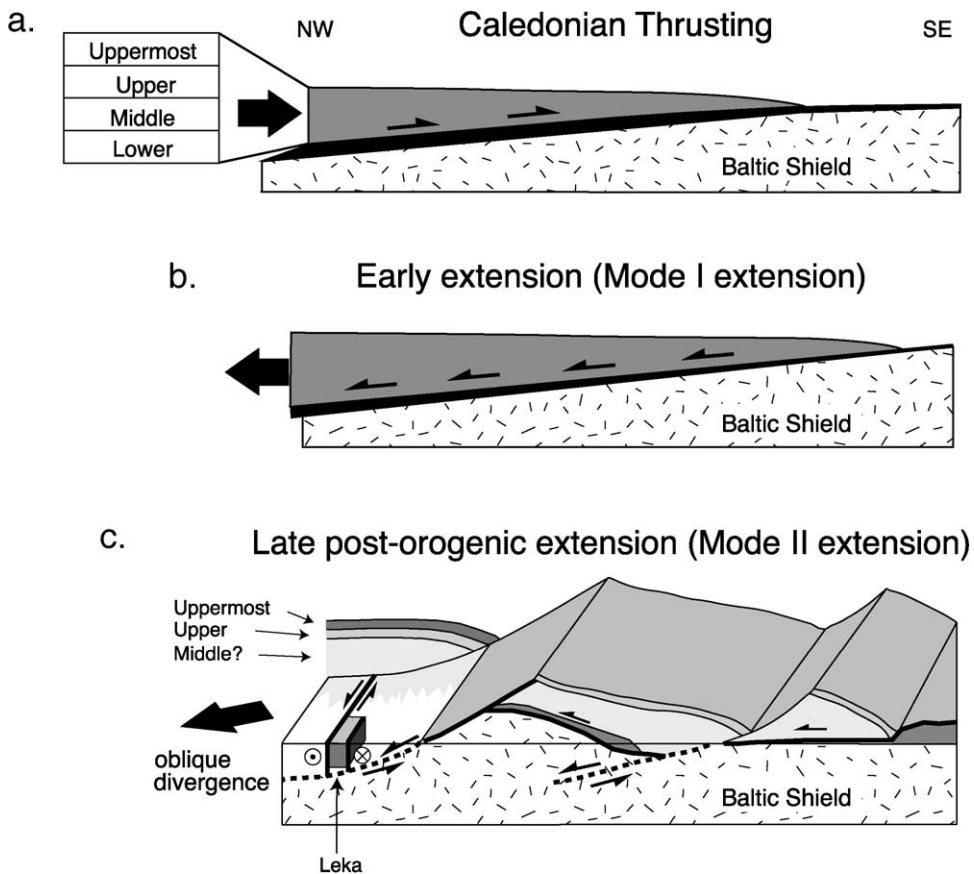


Fig. 7. Cartoon of the three stages of development of the Norwegian Caledonides. Caledonian thrusting (a) is followed by reactivation of thrust sheets in extension (b—Mode I extension). (c) Three-dimensional cartoon of strike-slip partitioning in an obliquely divergent setting. Late-stage deformation accommodated on high-angle, listric normal faults (Mode II), while transcurrent motion occurs on coast-parallel strike-slip faults. Modified from Fossen (1992).

Grønlie and Roberts, 1989; Torsvik et al., 1989). In contrast, Gabrielsen and Robinson (1984) suggest that dextral motion occurs on NE–SW fractures during the Late Jurassic, opposite to the motion recorded on similarly oriented features on Leka. Dextral motion is also recorded on the Møre–Trøndelag fault zone during the Mesozoic Era (Fossen, 1989; Grønlie and Roberts, 1989; Torsvik et al., 1989). Consequently, the margin-parallel, sinistral displacement displayed on Leka probably formed in response to obliquely divergent plate motion during late orogenic extension.

#### 5.4. Regional context and possible models of postorogenic extension

Multiple authors have discussed margin-parallel, strike-slip motion during the Late Paleozoic Era and how it relates to orogenic extension (Buckovics et al., 1984; Grønlie and Roberts, 1989; Torsvik et al., 1989; Séranne, 1992). However, these studies are mainly

from southern Norway and the process of orogenic extension is less well studied north of the Møre–Trøndelag fault zone.

In southern Norway, Fossen (1992, 2000) recognized two distinct styles of orogenic extension (Fig. 7). The earlier style (Mode I) involved extensional reactivation of the contractional thrust faults (e.g., extensional backsliding). The later Mode II style of extension involves the formation of higher-angle normal faults. These west- and northwest-dipping faults allow the juxtaposition of lower and higher units of the nappe stacks. In map view, significantly lower units of the nappe stack may be exposed immediately east of the higher units along these structures. The occurrence of Mode II structures was confirmed by seismic profiling offshore western Norway (Hurich et al., 1989).

If high-angle (Mode II) normal faults occur in central Norway, then there is a component of margin-parallel, strike-slip motion that is not presently

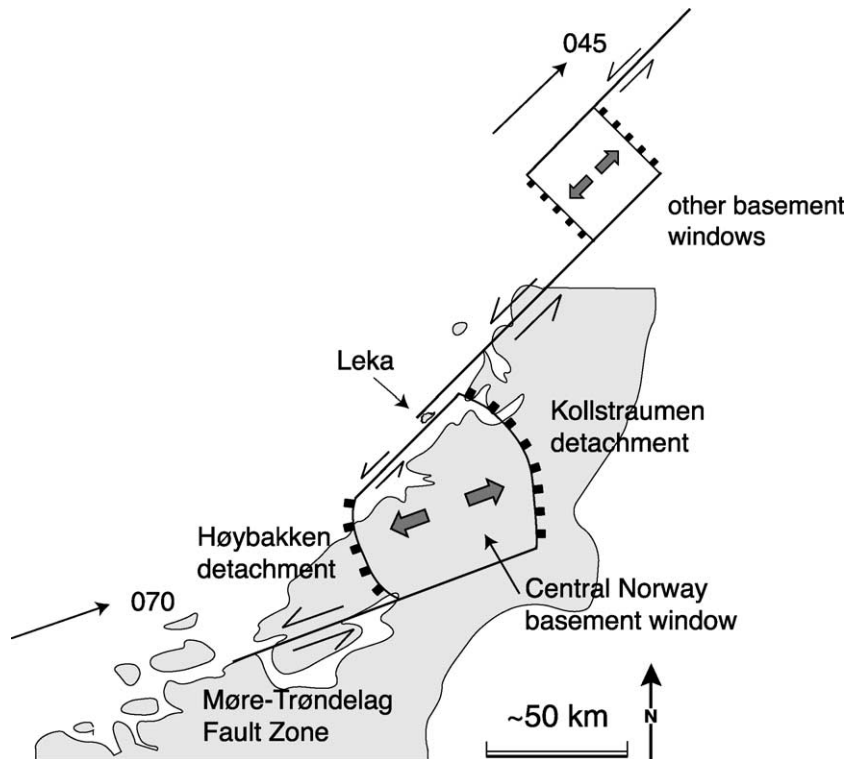


Fig. 8. Two-dimensional cartoon of sinistral faulting occurring simultaneously with domal uplift of the allochthonous basement. A series of left-lateral en echelon faults bound the domal basement uplifts and allow bidirectional extension of the nappe stacks that overly the domal uplifts. This model is broadly consistent with the model of Braathen et al. (2000).

accounted for in this model (Fig. 7). The Nord-Trøndelag region may respond to this obliquely divergent motion by strike-slip partitioning, where motion is kinematically distributed between normal faulting inland and strike-slip faulting offshore. Similar kinematic partitioning occurs in obliquely convergent settings, such as the San Andreas fault system in central California, with simultaneous activation of thrust and strike-slip faults (Tikoff and Teyssier, 1994). Although strike-slip partitioning is observed in obliquely divergent regimes in neotectonic settings (e.g., Gulf of California; Dorsey and Umhoefer, 2000), it is not commonly reported from ancient orogens. We relate this absence to result from their low preservation potential. These strike-slip structures are very likely to occur at the continental margin and therefore become buried or obliterated by subsequent rifting in late stages of the Wilson cycle.

Alternatively, Braathen et al. (2000) suggest that a distinct structural style occurs north of the Møre–Trøndelag fault zone, in the Central Norway Basement Window. Rather than the development of high-angle, Mode II normal faults, they argue that domal uplifts accommodate extension. Particularly addressing the Nord-Trøndelag region, these authors suggest that the basement gneisses exposed immediately east of Leka represent a domal uplift (Fig. 8). In their model, there is simultaneous, bidirectional movement of the nappe sheets structurally above the gneisses. To the northeast, movement is ENE directed (070), while to the southwest, movement is WSW directed (250).

If domal uplift is the main structural style in this region (Braathen et al., 2000; see, however, Fossen and Rykkelid, 1992; Rice, 2001), our study shows that there must also be a component of strike-slip faulting. The Central Norway Basement Window is potentially bounded on the north side by sinistral faults associated with the LOC, and on the south side by the margin parallel Møre–Trøndelag fault zone (Fig. 8). As both structures indicate sinistral motion during oblique divergence, the exposure of the basement-cored regions may be related to strike-slip tectonism.

Because of the preservation of the ultramafic LOC and its pull-apart geometry, it is clear that sinistral strike-slip motion occurs in the Nord-Trøndelag region of western Norway. This sinistral faulting

reflects a transcurrent component of obliquely divergent plate motion during orogenic extension. Consequently, in this region, postorogenic deformation is not exclusively the result of either Mode II extension or the domal uplift model.

## 6. Conclusions

The Leka Ophiolite Complex exists in a pull-apart structure, bounded by NE-oriented sinistral faults. A 25-mGal positive gravity anomaly is centered on the LOC. Inversion of gravity data, using a density contrast of 0.4 g/cm<sup>3</sup>, demonstrates a rhombochasm geometry for the LOC. The body has steep walls, a flat bottom located at 7 km depth, and all of the body lies underneath the present mapped surface exposure. The presence of a pull-apart explains the preservation of the Leka Ophiolite, which belongs to the highest thrust sheet in the Scandinavian Caledonides but is surrounded by rocks corresponding to lower tectonostratigraphic levels in the nappe stack.


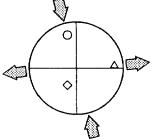
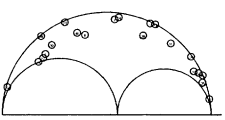
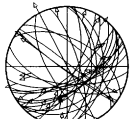
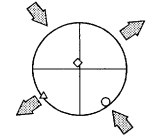
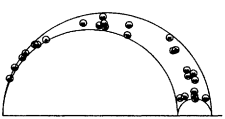
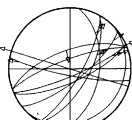
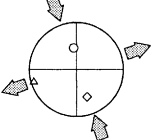
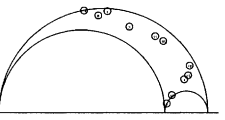
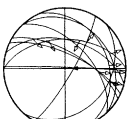
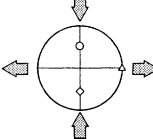
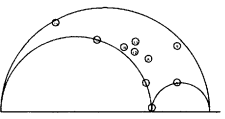
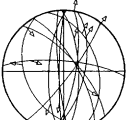
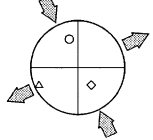
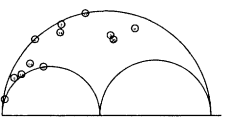

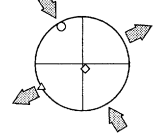
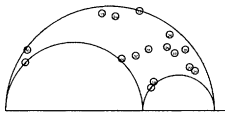
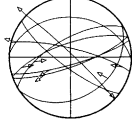
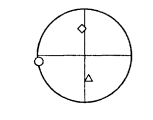
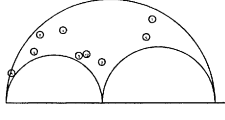
Paleostress tensors are consistent with sinistral movement on the NE-oriented bounding faults. There are two useful types of reduced paleostress tensors found on the island of Leka. One type, with 11 locations across the island, shows pure tension where the tension direction varies from E–W to NE–SW. A second type, with six sites exhibiting this behavior, had the same orientation for the tension direction and has an added component of N–S- to NNW–SSE-directed compression. The existence of strike-slip deformation along the coast of Norway suggests the possibility that strike-slip partitioning was part of obliquely divergent motion during postorogenic extension in the Scandinavian Caledonides.

## Acknowledgements

This work was supported by a Fulbright Fellowship and a NSF Graduate Student Fellowship (SJT). B. Célérier graciously assisted us in the use of the paleostress inversion program. SJT would like to thank Steve Wojtal for sponsoring a senior thesis that ultimately led to this work. We thank A. Braathen and A.H. Rice for their very detailed and helpful reviews.

## Appendix A

The tables below show the results of paleostress analysis. The columns are defined as follows: *No.* is the station number. *N*, *%tot* shows the number of faults used in the inversion and the percentage of the total number of measured faults that these faults represent. *Faults and striae* show the lower hemisphere, equal area stereonet where faults are denoted as great circles and slickensides as arrows. The *stress tensor* column shows the principal axes of the stress tensor calculated using the method of Célérier (1999). These are plotted on equal area stereonet where the circle is  $\sigma_1$ , the diamond is  $\sigma_2$  and the triangle is  $\sigma_3$ . The *Mohr circle* column displays the upper half of a three-dimensional Mohr circle with the fault data given by the small, unfilled circles. The tensor aspect ratio *R* is defined in the text. The *comments* column contains the orientations of the principal axes of the calculated stress tensor that best describes the majority of the data, given as a bearing/plunge.

No.	N, % tot.	Faults & Striae	Stress Tensor	Mohr Circle	R	Comments
122, 123	N=22 50% of dark green, 31% of total				0.493	$\sigma_1=348.7 / 22.6$ $\sigma_2=216.5 / 58.2$ $\sigma_3=87.9 / 21.1$ for dark green serpentine slickensides
121	N=28 36%				0.163	$\sigma_1=142.3 / 10.8$ $\sigma_2=241.1 / 78.6$ $\sigma_3=233.0 / 3.6$
120	N=11 58%				0.21	$\sigma_1=352.3 / 51.8$ $\sigma_2=158.9 / 37.4$ $\sigma_3=253.9 / 6.5$
118	N=11 69%				0.28	$\sigma_1=359.1 / 46.2$ $\sigma_2=180.6 / 43.8$ $\sigma_3=89.9 / 0.8$
135	N=12 60%				0.531	$\sigma_1=343.3 / 37.0$ $\sigma_2=142.7 / 51.2$ $\sigma_3=245.5 / 10.2$
110	N=16 43%				0.343	$\sigma_1=330.5 / 9.9$ $\sigma_2=149.3 / 80.1$ $\sigma_3=240.5 / 0.2$
116	N=9 75%				0.590	$\sigma_1=266.1 / 3.5$ $\sigma_2=359.0 / 40.4$ $\sigma_3=172.0 / 49.4$

No.	N, % tot.	Faults & Striae	Stress Tensor	Mohr Circle	R	Comments
115	N=11 92%				0.790	$\sigma_1=282.6 / 19.7$ $\sigma_2=176.0 / 38.6$ $\sigma_3=33.4 / 44.8$
113	N=14 88%				0.759	$\sigma_1=330.8 / 20.4$ $\sigma_2=76.7 / 36.5$ $\sigma_3=217.8 / 46.5$
117	N=11 48%				0.65	$\sigma_1=108.2 / 21.1$ $\sigma_2=355.0 / 45.5$ $\sigma_3=215.1 / 36.9$
132	N=28 61%				0.267	$\sigma_1=200.8 / 50.6$ $\sigma_2=327.4 / 26.1$ $\sigma_3=72.0 / 27.2$
129	N=22 54%				0.375	$\sigma_1=245.3 / 44.2$ $\sigma_2=346.7 / 7.5$ $\sigma_3=80.2 / 44.8$
128	N=18 62%				0.745	$\sigma_1=158.8 / 37.5$ $\sigma_2=51.8 / 20.9$ $\sigma_3=259.3 / 45.2$
127	N=16 55%				0.151	$\sigma_1=183.0 / 90.3$ $\sigma_2=333.8 / 8.0$ $\sigma_3=64.4 / 3.7$
124	N=26 81%				0.339	$\sigma_1=22.2 / 77.9$ $\sigma_2=195.5 / 12.0$ $\sigma_3=285.8 / 1.4$
125	N=10 71%				0.94	$\sigma_1=34.1 / 48.3$ $\sigma_2=174.0 / 34.2$ $\sigma_3=278.9 / 20.8$
122, 123	N=11 92% of calcite, 16% of total				0.395	$\sigma_1=314.1 / 79.1$ $\sigma_2=150.3 / 10.5$ $\sigma_3=59.8 / 3.0$ calcitic slickensides



No.	N, % tot.	Faults & Striae	Stress Tensor	Mohr Circle	R	Comments
122, 123	N=9 64% of light green, 13% of total				0.102	$\sigma_1=312.6 / 76.9$ $\sigma_2=130.7 / 13.1$ $\sigma_3=220.8 / 0.4$ light green serpentinite slickensides
130	N=18 69%				0.403	$\sigma_1=248.0 / 68.0$ $\sigma_2=149.6 / 3.4$ $\sigma_3=58.3 / 21.7$
131	N=16 55%				0.560	$\sigma_1=250.7 / 67.1$ $\sigma_2=354.9 / 5.9$ $\sigma_3=87.3 / 22.1$
136	N=11 58%				0.160	$\sigma_1=153.0 / 59.4$ $\sigma_2=339.7 / 30.5$ $\sigma_3=248.0 / 3.0$
119	N=9 56%				0.333	$\sigma_1=216.7 / 61.1$ $\sigma_2=325.0 / 9.8$ $\sigma_3=60.0 / 26.9$
138	N=38 88%				0.386	$\sigma_1=34.9 / 67.9$ $\sigma_2=183.9 / 19.2$ $\sigma_3=277.6 / 10.5$
139	N=26 87%				0.091	$\sigma_1=22.2 / 79.9$ $\sigma_2=195.5 / 12.0$ $\sigma_3=285.8 / 1.4$

## References

- Améglio, L., Vignerresse, J.L., Bouchez, J.L., 1996. An assessment of combined fabrics and gravity data in granites. In: Bouchez, J.L., Hutton, D., Stephens, W.E. (Eds.), *Granite: from Melt Segregation to Emplacement Fabrics*. Kluwer Academic Publisher, Amsterdam, pp. 199–214.
- Andersen, T.B., 1998. Extensional tectonics in the Caledonides of southern Norway, an overview. *Tectonophysics* 285, 333–351.
- Angelier, J., 1975. Sur l'analyse de mesures recueillies dans des sites faillés: l'utilité d'une confrontation entre les méthodes dynamiques et cinématiques. *Comptes Rendus de l'Académie des Sciences, Paris D* 281, 1805–1808 (Erratum: *Ibid (D)* 1976, 283, 466).
- Angelier, J., 1984. Tectonic analysis of fault slip data sets. *Journal of Geophysical Research* 89, 5835–5848.
- Angelier, J., 1989. From orientation to magnitudes in paleostress determinations using fault slip data. *Journal of Structural Geology* 11, 37–50.
- Angelier, J., 1994. Fault slip analysis and palaeostress reconstruction. In: Hancock, P.L. (Ed.), *Continental Deformation*. Pergamon, Tarrytown, pp. 53–100.
- Angelier, J., Tarantola, A., Vallette, B., Manoussis, S., 1982. Inversion of field data in fault tectonics to obtain the regional stress.

- Single phase fault populations: a new method of compute the stress tensor. *Geophysical Journal of the Royal Astronomical Society* 69, 607–621.
- Aydin, A., Nur, A., 1982. Evolution of pull-apart basins and their scale independence. *Tectonics* 1, 91–105.
- Bott, M.H.P., 1959. The mechanics of oblique slip faulting. *Geological Magazine* 96, 109–117.
- Braathen, A., 1999. Kinematics of post-Caledonian polyphase brittle faulting in the Sunnfjord region, western Norway. *Tectonophysics* 302, 99–121.
- Braathen, A., Nordgulen, Ø., Osmundsen, P.T., Andersen, T.B., Solli, A., Roberts, D., 2000. Devonian, orogen-parallel, opposed extension in the central Norwegian Caledonides. *Geology* 28, 615–618.
- Braathen, A., Nordgulen, Ø., Osmundsen, P.T., Andersen, T.B., Solli, A., Roberts, D., 2000. Devonian, orogen-parallel, opposed extension in the central Norwegian Caledonides. Reply *Geology* 29, 375–376.
- Buckovics, C., Cartier, E.G., Shaw, N.D., Ziegler, P.A., 1984. Structure and development of the mid-Norway continental margin. In: Spencer, A.M., Johnsen, S.O., Moerk, A., Nysaether, E., Songstad, P., Spinnangr, A. (Eds.), *Petroleum Geology of the North European Margin*. Graham and Trotman, London, pp. 407–423.
- Célérier, B., 1988. How much does slip on a reactivated fault plane constrain the stress tensor? *Tectonics* 7, 1257–1278.
- Célérier, B., 1999. FSA: Fault Slip Analysis software, <http://www.isteeem.univ-montp2.fr/PERSO/celerier/software/fsa.html>.
- Cordell, L., Henderson, R.G., 1968. Iterative three dimensional solution of gravity anomaly using a digital computer. *Geophysics* 33, 596–601.
- Dorsey, R.J., Umhoefer, P.J., 2000. Tectonic and eustatic controls on sequence stratigraphy of the Pliocene Loreto Basin, Baja California Sur, Mexico. *Geological Society of America Bulletin* 112, 177–199.
- Dunning, G.R., Pedersen, R.B., 1988. U/Pb ages of ophiolites and arc-related plutons of the Norwegian Caledonides. Implications for the development of Iapetus. *Contributions to Mineralogy and Petrology* 98, 13–23.
- Etchecopar, A., Vasseur, G., Daignieres, M., 1981. An inverse problem in microtectonics for the determination of stress tensors from fault striation analysis. *Journal of Structural Geology* 3, 51–65.
- Fossen, H., 1989. Indication of transpressional tectonics in the gullfaks oil-field, northern North Sea. *Marine and Petroleum Geology* 6, 22–30.
- Fossen, H., 1992. The role of extensional tectonics in the Caledonides of South Norway. In: Burg, J.P., Mainprice, D., Petit, J.P. (Eds.), *Mechanical Instabilities in Rocks and Tectonics; a Selection of Papers*. *Journal of Structural Geology*, vol. 14, pp. 1033–1046.
- Fossen, H., 2000. Extensional tectonics in the Caledonides; synorogenic or postorogenic? *Tectonics* 19, 213–224.
- Fossen, H., Rykkelid, E., 1992. Postcollisional extension of the Caledonide Orogen in Scandinavia; structural expressions and tectonic significance. *Geology* 20, 737–740.
- Furnes, H., Pedersen, R.B., Stillman, C.J., 1988. The Leka Ophiolite Complex, central Norwegian Caledonides: field characteristics and geotectonic significance. *Journal of the Geological Society of London* 145, 401–412.
- Gabrielsen, R.H., Robinson, C., 1984. Tectonic inhomogeneities of the Kristiansund–Bodoie fault complex, offshore mid-Norway. In: Spencer, A.M., Johnsen, S.O., Moerk, A., Nysaether, E., Songstad, P., Spinnangr, A. (Eds.), *Petroleum Geology of the North European Margin*. Graham and Trotman, London, pp. 397–406.
- Gabrielsen, R.H., Faereth, R., Hamar, G., Roennevik, H., 1984. Nomenclature of the main structural features on the Norwegian continental shelf north of the 62nd parallel. In: Spencer, A.M., Johnsen, S.O., Moerk, A., Nysaether, E., Songstad, P., Spinnangr, A. (Eds.), *Petroleum Geology of the North European Margin*. Graham and Trotman, London, pp. 41–60.
- Gabrielsen, R.H., Odinsen, T., Grunnaleite, I., 1999. Structuring of the northern Viking Graben and the Møre Basin: the influence of basement structural grain, and the particular role of the Møre–Trøndelag fault complex. *Marine and Petroleum Geology* 16, 443–465.
- Gronlie, A., Roberts, D., 1989. Resurgent strike-slip duplex development along the Hitra–Snåsa and Verran faults, Møre–Trøndelag fault zone, central Norway. *Journal of Structural Geology* 11, 295–305.
- Gronlie, A., Naeser, C.W., Naeser, N.D., Mitchell, J.G., Sturt, B.A., Ineson, P.R., 1994. Fission-track and K–Ar dating of tectonic activity in a transect across the Møre–Trøndelag fault zone, central Norway. *Norsk Geologisk Tidsskrift* 74, 24–34.
- Hancock, P.L., 1985. Brittle microtectonics: principles and practice. *Journal of Structural Geology* 7, 437–457.
- Hibbard, J., 1983. *Geology of the Bare Verte Peninsula, Newfoundland*. Mineral Development Division, Department of Mines and Energy, Government of Newfoundland and Labrador Memoir 2.
- Hossack, J.R., Cooper, M.A., 1986. Collision tectonics in the Scandinavian Caledonides. In: Coward, M.P., Ries, A.C. (Eds.), *Collision Tectonics*, vol. 19. Geological Society, London, pp. 287–304, Special Publications.
- Hurich, C.A., Palm, H., Dyrelus, D., Kristoffersen, Y., 1989. Deformation of the Baltic continental crust during Caledonide intracontinental subduction: views from seismic reflection data. *Geology* 7, 423–425.
- Krabbendam, M., Dewey, J.F., 1998. Exhumation of UHP rocks by transtension in the Western Gneiss Region, Scandinavian Caledonides. In: Holdsworth, R.E., Strachan, R.A., Dewey, J.F. (Eds.), *Continental Transpressional and Transtensional Tectonics*, vol. 135. Geological Society, London, pp. 159–181, Special Publications.
- Mann, P., Gordon, M.B., 1996. Tectonic uplift and exhumation of blueschist belts along transpressional strike-slip fault zones. In: Bebout, G.E., Scholl, D.W., Kirby, S.H., Platt, J.P. (Eds.), *Subduction Top to Bottom*. Geophysical Monograph, vol. 96. American Geophysical Union, Washington, DC, pp. 143–154.
- Michael, A.J., 1984. Determination of stress from slip data: faults and folds. *Journal of Geophysical Research* 89, 11517–11526.
- Milnes, A.G., Wennberg, O.P., Skår, Ø., Koestler, A.G., 1997. Contraction, extension and timing in the South Norwegian Caledonides: the Sognefjord transect. In: Burg, J.-P., Ford, M. (Eds.),

- Orogeny Through Time, vol. 121. Geological Society, London, pp. 123–148, Special Publication.
- Nemcock, M., Lisle, R.J., 1995. A stress inversion procedure for polyphase fault/slip data. *Journal of Structural Geology* 17, 1445–1453.
- Osmundsen, P.T., Andersen, T.B., 2001. The middle Devonian basins of western Norway: sedimentary response to large-scale transtensional tectonics? *Tectonophysics* 332, 51–68.
- Osmundsen, P.T., Andersen, T.B., Markussen, S., Svenby, A.K., 1998. Tectonics and sedimentation in the hangingwall of a major extensional detachment; the Devonian Kvamshesten Basin, western Norway. *Basin Research* 10, 213–234.
- Peacock, D.C.P., Sanderson, D.J., 1995. Pull-aparts, shear fractures and pressure solution. *Tectonophysics* 241, 1–13.
- Pedersen, R.B., 1986. The nature and significance of magma chamber margins in ophiolites: examples from the Norwegian Caledonides. *Earth and Planetary Science Letters* 77, 100–112.
- Pedersen, R.B., Furnes, H., Dunning, G., 1988. Some Norwegian ophiolite complexes reconsidered. *Norges Geologisk Undersøkelse* 3, 80–85, Special Publication.
- Petit, J.P., 1987. Criteria for the sense of movement on fault surfaces in brittle rocks. *Journal of Structural Geology* 9, 597–608.
- Prestvik, T., 1972. Alpine-type mafic and ultramafic rocks of Leka, Nord-Trøndelag. *Norges Geologisk Undersøkelse* 273, 23–34.
- Reches, Z., 1987. Determination of the tectonic stress tensor from slip along faults that obey the Coulomb yield criterion. *Tectonics* 6, 849–861.
- Rice, A.H.N., 2001. Devonian, orogen-parallel, opposed extension in the central Norwegian Caledonides: comment. *Geology* 29, 374.
- Roberts, D., Gee, D.G., 1985. An introduction to the structure of the Scandinavian Caledonides. In: Gee, D.G., Sturt, B.A. (Eds.), *The Caledonide Orogen—Scandinavia and Related Areas*. Wiley, Chichester, pp. 55–68.
- Séranne, M., 1992. Late Paleozoic kinematics of the Møre–Trøndelag Fault Zone and adjacent areas, central Norway. *Norsk Geologisk Tidsskrift* 72, 141–158.
- Sindre, A., Pedersen, R.B., 1990. Gravimetrisk undersøkelse av Leka ofiolittkompleks. *Norges Geologiske Undersøkelse, Rapport nr. 90.152*, 20 pp.
- Solli, A., Bugge, T., Thorsnes, T., 1997. *Geologisk kart over Norge, berggrunskart NAMSOS, M 1:250,000*. Norges Geologiske Undersøkelse.
- Steel, R., Siedlecka, A., Roberts, D., 1985. The Old Red Sandstone basins of Norway and their deformation: a review. In: Gee, D.G., Sturt, B.A. (Eds.), *The Caledonide Orogen—Scandinavia and Related Areas*. Wiley, Chichester, pp. 293–315.
- Sturt, B.A., Andersen, T.B., Furnes, H., 1985. The Skei Group, Leka: an unconformable clastic sequence overlying the Leka Ophiolite. In: Gee, D.G., Sturt, B.A. (Eds.), *The Caledonide Orogen—Scandinavia and Related Areas*. Wiley, Chichester, pp. 395–405.
- Sylvester, A.G., 1988. Strike-slip faults. *Geological Society of America Bulletin* 100, 1666–1703.
- Terry, M.P., Robinson, P., Hamilton, M.A., Jercinovic, M.J., 2000. Monazite geochronology of UHP and HP metamorphism, deformation, and exhumation, Nordoyane, Western Gneiss region, Norway. *American Mineralogist* 85, 1651–1664.
- Tikoff, B., Teyssier, C., 1992. Crustal-scale, en echelon “P-shear” tensional bridges: a possible solution to the batholithic room problem. *Geology* 20, 927–930.
- Tikoff, B., Teyssier, C., 1994. Strain modeling of displacement-field partitioning in transpressional orogens. *Journal of Structural Geology* 16, 1575–1588.
- Torsvik, T.H., Sturt, B.A., Ramsay, D.M., Grønlie, A., Roberts, D., Smethurst, M., Atakan, K., Bøe, R., Walderhaug, H.J., 1989. Paleomagnetic constraints on the early history of the Møre–Trøndelag Fault Zone. In: Kissel, C., Laj, C. (Eds.), *Paleomagnetic Rotations and Continental Deformation*. Kluwer Academic Publishers, Dordrecht, pp. 431–457.
- Twiss, R.J., Unruh, J.R., 1998. Analysis of fault slip inversions: do they constrain stress or strain rate? *Journal of Geophysical Research* 103, 12205–12222.
- Vigneresse, J.L., 1990. Use and misuse of geophysical data to determine the shape at depth of granitic intrusions. *Geological Journal* 25, 248–260.
- Wallace, R.E., 1951. Geometry of shearing stress and relation to faulting. *Journal of Geology* 59, 118–130.
- Will, T.M., Powell, R., 1991. A robust approach to the calculation of paleostress fields from fault plane data. *Journal of Structural Geology* 13, 813–821.
- Wojtal, S., 2001. The nature and origin of asymmetric arrays of shear surfaces in fault zones. In: Holdsworth, R.E., Strachan, R.A., Magloughlin, J.F., Knipe, R.J. (Eds.), *The Nature and Tectonic Significance of Fault Zone Weakening*, vol. 86. Geological Society, London, pp. 171–193, Special Publication.
- Wojtal, S., Pershing, J., 1991. Paleostresses associated with faults of large offset. *Journal of Structural Geology* 13, 49–62.